Available online at www.sciencedirect.com
SCIENCE DIRECT®
ELSEVIER
Materials Letters 57 (2003) 3186–3192
MATERIALS LETTERS
www.elsevier.com/locate/matlet

Sol–gel synthesis and characterization of V_2O_5 powders

M. Gotić[a], S. Popović[b], M. Ivanda[a], S. Musić[a,*]

[a] *Division of Materials Chemistry, Rudjer Bošković Institute, P.O. Box 180 Bijenicka Cesta 54, HR-10002 Zagreb, Croatia*
[b] *Faculty of Sciences, Department of Physics, University of Zagreb, P.O. Box 331, HR-10002 Zagreb, Croatia*

Received 23 December 2002; accepted 28 December 2002

Abstract

V_2O_5 particles were precipitated by the sol–gel method, then subjected to heat treatment. Samples were analyzed using XRD, TGA/DTA, FT-IR, Raman and transmission electron microscopy (TEM) techniques. XRD showed an amorphous-like structure of these particles with the beginning of their crystallization, whereas TEM showed their fibrillar morphology. In the FT-IR spectrum of the starting sample, not all bands typical of the crystalline V_2O_5 spectrum were developed. The Raman spectrum showed all bands of V_2O_5, however, with a significant broadening. The fibrillar morphology of V_2O_5 particles was disappearing with increase in the heating temperature, and at 600 °C, only big particles of irregular shape were obtained. Heating of the starting V_2O_5 particles in argon atmosphere up to 600 °C produced the V_3O_7 phase as associated with the predominant V_2O_5 phase.

Keywords: Sol–gel; V_2O_5; XRD; DTA; FT-IR; Raman; TEM

1. Introduction

Colloid chemistry of vanadium pentoxide (V_2O_5) has attracted many researches in the past few decades. V_2O_5 can be obtained in the form of gel or stable colloid particles. It belongs to a group of several examples of metal oxides, which form a periodic colloid structure in an aqueous medium. V_2O_5 has found various applications in sensor and electrochromic devices, lithium batteries, catalysts, etc.

Pelletier et al. [1] investigated (a) preparation of V_2O_5 gel by ion-exchange, (b) precipitation from peroxovanadic species and (c) reprecipitation from V_2O_5 powder suspended in water. V_2O_5 also reprecipitated after a prolonged aging at room temperature in the system V_2O_5–NH_3–H_2O, showing a specific fibrillar morphology [2]. Investigation of V_2O_5 gels by electron microscopy [3] and XRD [4] showed the formation of V_2O_5 ribbons as a product of the polymerization of vanadium hydroxy species. Hirashima et al. [5] investigated the effects of aging and drying on the structure of V_2O_5 gels, prepared by alkoxide route with and without GeO_2 (up to 10 mol%). Crystalline V_2O_5 was not detected in xerogel and aerogel powders produced by this method. V_3O_7 crystallized in "wet" gels under supercritical conditions in ethanol at 250 °C and 210 atm.

Crystalline V_2O_5 films were prepared [6] by reactive d.c. magnetron sputtering onto ITO-coated glass, glass slides or Be foil. Lithium ions were inserted

* Corresponding author.
E-mail address: music@rudjer.irb.hr (S. Musić).

0167-577X/03/$ - see front matter © 2003 Elsevier Science B.V. All rights reserved.
doi:10.1016/S0167-577X(03)00022-3

electrochemically into V_2O_5 to produce $Li_xVO_{2.5}$, $0<x<1.5$. Lithium intercalation induced changes in the optical absorption spectrum, as well as in the EMF of $Li_xVO_{2.5}$/Li cells. Meulenkamp et al. [7] showed that the intercalation of lithium ions influenced structural changes in $Li_xV_2O_5$ films in dependence on x value. Özer [8] prepared V_2O_5 films by the spin coating method and also investigated lithiation of these films. The investigated films were stable in the switching between oxidized and reduced states for at least 600 cycles.

Supported V_2O_5 catalysts are of great importance for the selective oxidation of hydrocarbons, as well as for the selective catalytic reduction of NO_x gases. Raman spectroscopy was used to identify changes in the structure of dispersed V_2O_5 in dependence on its loading and the nature of the substrate [9,10].

In the present work we have focused on the synthesis and characterization of V_2O_5 powders using the sol–gel method. This method was mainly utilized in the preparation of V_2O_5 films. However, there is a difference between the formation of V_2O_5 films, due to the surface effect of the substrate, and V_2O_5 powders. In comparison with the traditional "wet" procedures, the sol–gel method by alkoxide route is very sensitive to experimental conditions. In the present work the sol–gel synthesis of V_2O_5 was performed under well-defined experimental conditions.

2. Experimental

Vanadium (V)-triisopropoxide oxide (95–99%), $VO[CHO(CH_3)_2]_3$, supplied by Alfa Aesar®, and isopropanol, $(CH_3)_2CHOH$, by Aldrich, were used as received. Water obtained from the Milli-Q purified system was used.

The synthesis was performed in an oil bath using a specially designed all-glass assembly, which consists of a round-bottomed boiling glass flask with four necks, glass mixer, water condenser, inlet glass tube to perform N_2 bubbling and one ground outer glass joint used for the addition of reagents. The glass mixer was connected at the outer center neck joint of the flask; it consisted of a specially designed glass adapter fixed on the mixer and filled with silicon oil in order to prevent any contact between air moisture and the reaction flask. Before bubbling N_2 gas into the reaction vessel, extra pure N_2 was additionally purified through a pyrogallol trap, concentrated H_2SO_4 bubbler and then through two tubes with silica gel. The experiment started by adding chemicals in this order: isopropanol (187 ml), vanadium (V)-triisopropoxide (25 g) and water (25 ml). The solution in the reaction vessel was refluxed and stirred constantly at 500–1000 rpm in nitrogen atmosphere. After 100 min of hydrolysis at 70 °C, the so formed "frozen" gel was resuspended in an ultrasonic bath for 10 min to release trapped water. Thus obtained "liquefied gel" was poured into a Petri dish and dried at 60 °C. The experimental conditions for the synthesis and the flow chart of the preparation procedure for V_2O_5 samples are given in Table 1 and Flow chart 1.

X-ray powder diffraction patterns were taken at room temperature using a Philips counter diffractometer, model MPD 1880 (CuKα radiation, graphite monochromator, proportional counter).

The Raman scattering experiments were performed using a standard instrumental technique. A Coherent Innova-100 laser with $\lambda = 514.5$ nm served as an excitation source and the scattered light was analyzed with a DILOR Z-24 Raman spectrometer. The energy of the used laser beam was decreased in

Table 1
Conditions of the thermal treatment of the samples and the results of XRD analysis

Sample	Temperature of heating (°C)	Heating time (h)	Atmosphere	XRD analysis (approximate molar fraction)	Remark
V0	Starting sample		air	amorphous[a]	
V1	240		air	V_2O_5	LBDL
V2	300	0.5	air	V_2O_5	LBDL
V3	300	2	air	V_2O_5	LBDL
V4	300	6	air	V_2O_5	LBDL
V5	350	2	air	V_2O_5	SDL
V6	600	2	air	V_2O_5	SDL
V7	600[b]		air (DTA)	V_2O_5	SDL
V8	600[b]		argon (DTA)	$V_2O_5(0.9)+V_3O_7(0.1)$	SDL

LBDL = little broadened diffraction lines.
SDL = sharp diffraction lines.
[a] A beginning of V_2O_5 crystallization.
[b] Heating in DTA equipment at the rate 10 °C min^{-1}.

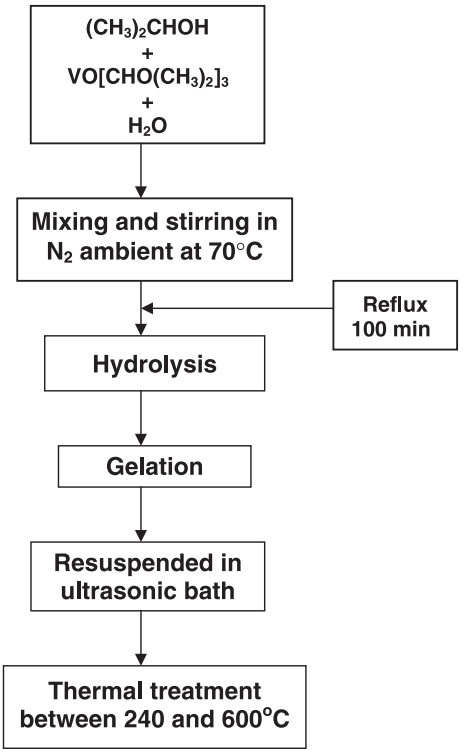

Flow chart 1. Flow chart of the procedure for preparation of V_2O_5 powders.

order to prevent its influence on possible V_2O_5 crystallization (recrystallization) during the measurements.

The FT-IR spectra were recorded at room temperature using a Perkin-Elmer spectrometer (model 2000). The Infrared Data Manager (IRDM) program, supplied by Perkin-Elmer, was used to process the spectra. The FT-IR spectra of the samples pressed into KBr pellets were collected in the wave number range of 4000–400 cm^{-1} (mid IR region) using the KBr beam splitter. Powder samples measured in the wave number range of 700–100 cm^{-1} (far IR region) were gently mixed with spectroscopic pure polyethylene powder, pressed into pellets and recorded in a compartment purged with extra pure nitrogen using a Mylar beam splitter. At least 100 scans with a resolution of 4 cm^{-1} in the far IR region were accumulated.

Thermal analysis was performed using an instrument manufactured by Netzsch. The temperature was controlled by a Pt–PtRh (10%) thermocouple, by applying a heating rate of 10 °C min^{-1} (DTA) and 5 °C min^{-1} (TGA).

Transmission electron microscopy (TEM) was performed using an EM-10 Opton electron microscope.

3. Results and discussion

Fig. 1 shows DTA curves of the starting sample, recorded in air and argon. The sample heated in air shows a very broad endothermic peak at 160 °C, which can be ascribed to the loss of water. Two exothermic peaks at 260 and 295 °C can be assigned to the V_2O_5 recrystallization in two steps, with additional removal of hydroxylated water. XRD analysis of the samples heated in air between 240 and 300 °C showed the presence of crystalline V_2O_5 (Table 1). A similar feature of the DTA curve was obtained in argon, and the only change was a shift of the exothermic peak from 295 to 320 °C. An XRD analysis of the sample obtained in argon showed V_2O_5 and a small amount of V_3O_7 due to reduction conditions. Fig. 2 shows XRD patterns of selected samples indicating an increase in the sharpness of diffraction lines of V_2O_5 and an increase in crystallite size from several nm up to several tens of nm with the increase in heating temperature.

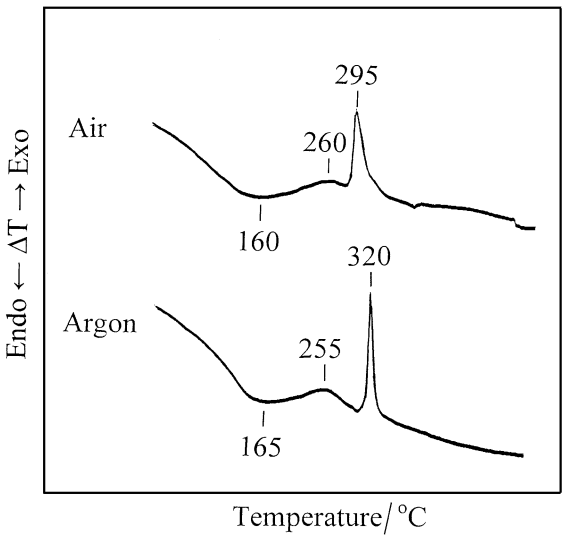

Fig. 1. DTA curves of starting sample V0, recorded in air and argon.

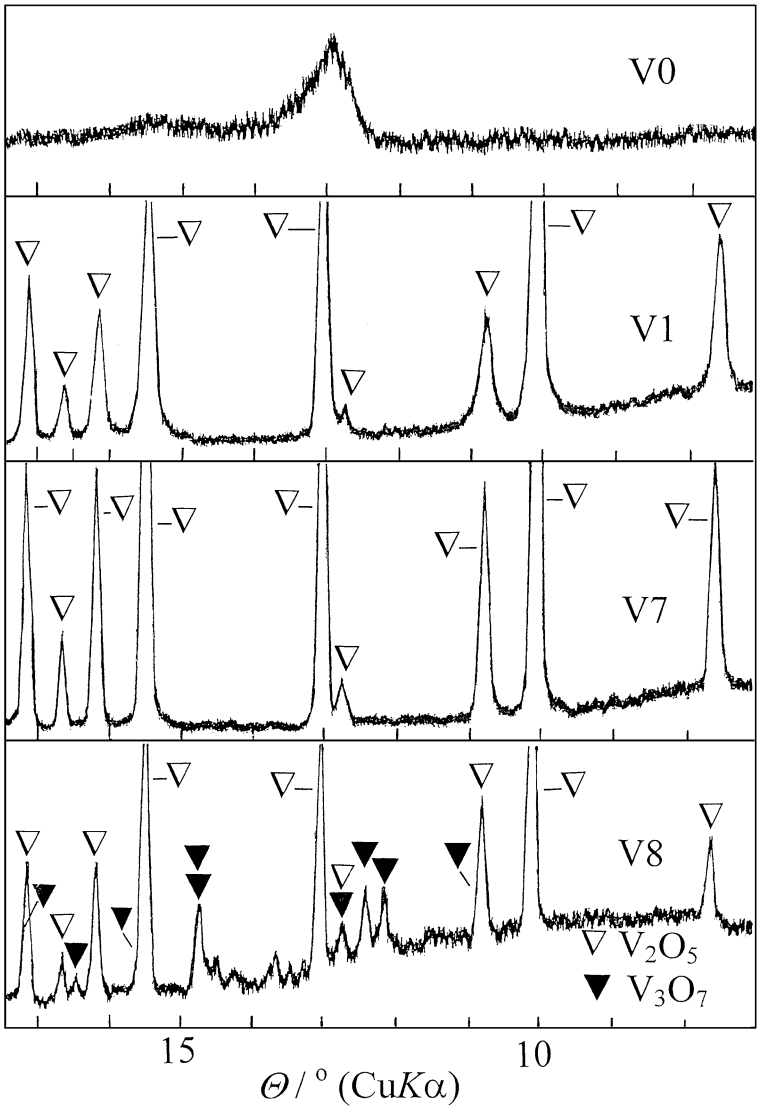

Fig. 2. Characteristic parts of XRD patterns of samples V0, V1, V7 and V8, recorded at room temperature.

Fig. 3a shows a TEM photograph of sample V0, indicating fine fibrillar morphology. This morphology disappeared with the increase in heating temperature (Fig. 3b), and upon heating at 600 °C, big V_2O_5 particles of irregular shape were produced (Fig. 3c). With a further increase in the heating temperature, the V_2O_5 glass transition occurred at 680 °C.

Kittaka et al. [11] prepared vanadium pentoxide hydrate ($V_2O_5{\cdot}nH_2O$) by polymerizing decavanadic acid obtained by a cation exchange reaction of the NH_4VO_3 solution in an ion exchange column. The thermal desorption spectrum of $V_2O_5{\cdot}nH_2O$ showed three peaks at 90, 180 and 325 °C. The first peak is assigned to sorbed O_2, whereas two other peaks are assigned to the removal of water. Kittaka et al. [12] also prepared fine spheres of V_2O_5 in O_2-H_2 flame at 2000 °C and observed that the particles contained hydrated V_2O_5 inside their microstructure, probably of the composition of $V_2O_5{\cdot}1.6H_2O$. The FT-IR spectra of V_2O_5 spheres evacuated at increasing

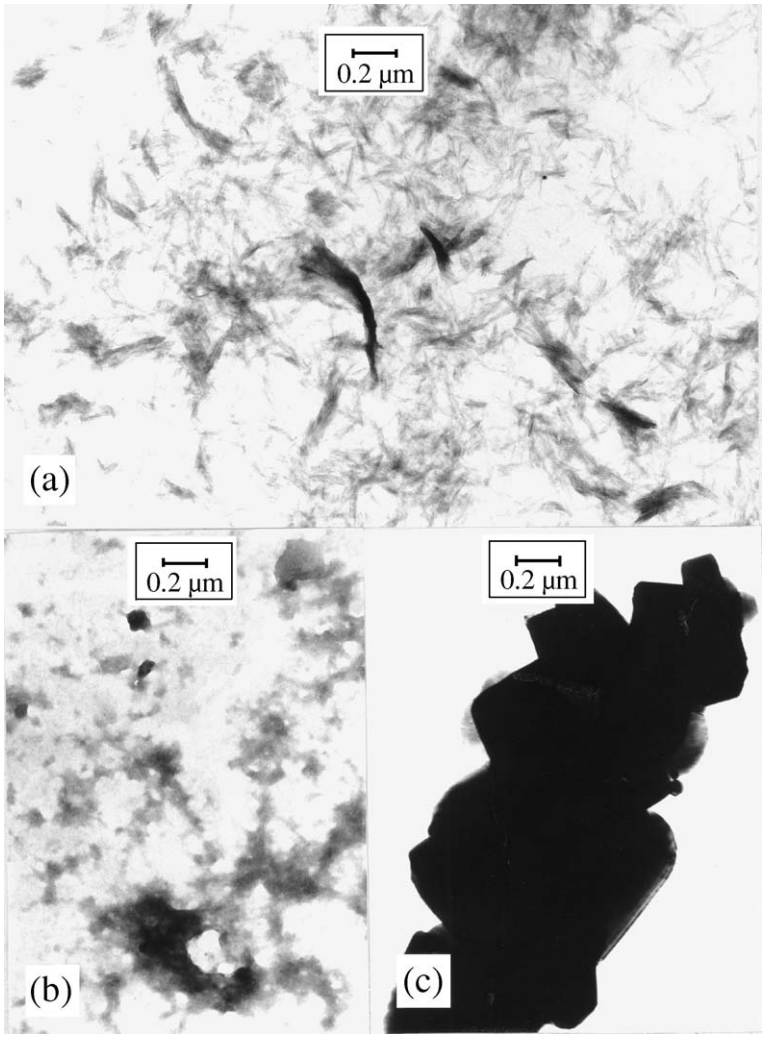

Fig. 3. TEM photographs of samples (a) V0, (b) V1 and V7.

temperature showed a decrease in the bands at 3350 and 1600 cm^{-1} on heating above 200 °C, which can be ascribed to the removal of H_2O molecules.

Figs. 4–6 show the FT-IR spectra of selected samples. The FT-IR spectrum of the starting sample shows main features of the V_2O_5 spectrum; however, not all bands typical of crystalline V_2O_5 were developed. Clauws et al. [13,14] measured the reflectance IR spectra on a single V_2O_5 crystal, as well as the transmittance spectra for V_2O_5 powder. For polycrystalline V_2O_5 pellets, the measured bands were classified as follows: active IR at 262, 370, 472, 813 and 982 cm^{-1} for the B_{3u} mode, 1023 for B_{2u} mode, and 217, 294 and 605 cm^{-1} for B_{1u} mode. The starting sample V0 shows a very strong IR band at 1002 cm^{-1} and broad bands at 759 and 537 cm^{-1} with shoulders at 810 and 666 cm^{-1}. The IR bands at 1739, 1724, 1619, 1469 and 1403 cm^{-1} are due to the residual organics. Upon heating the starting sample at 240 °C, the changes in the corresponding spectrum were observed. For example, strong and broad bands at 837 and 634 cm^{-1} are formed. The formation of a shoulder at 986 cm^{-1} was also visible. The FT-IR spectrum of sample V0 recorded in the far IR region showed two dominant IR bands at 516 and 282 cm^{-1} and a weak band at

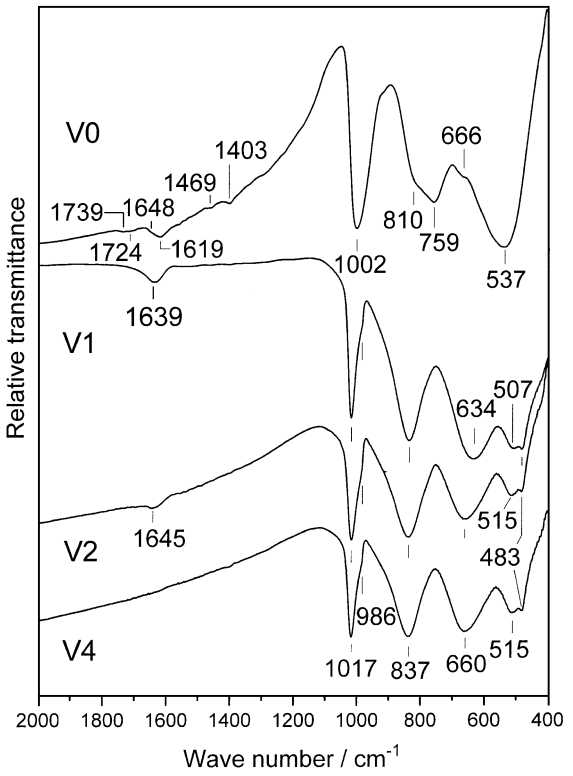

Fig. 4. FT-IR spectra of starting sample V0 and samples V1, V2 and V4. KBr matrix was used.

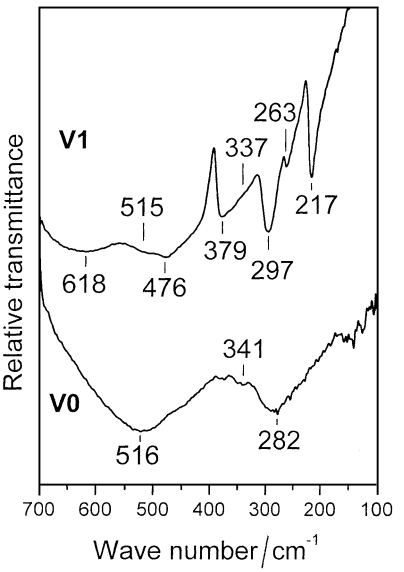

Fig. 5. FT-IR spectra of samples V0 and V1, recorded in the far IR region. Polyethylene matrix was used.

341 cm^{-1}. A difference in the reading of wave numbers for the same IR band are due to different matrices used, KBr in the mid IR region and polyethylene in the far IR region. Sample V1 showed in the far IR region the bands at 379, 297, 263 and 217 cm^{-1} and a shoulder at 337 cm^{-1}. The appearance of these IR bands is in line with the theoretical prediction. The FT-IR spectrum of sample V1 recorded in the mid IR region showed elimination of organic impurities; however, the water molecules were still present. Upon heating the starting sample at 300 °C for 6 h (sample V4), the water molecules (bending vibration at 1645 cm^{-1}) could not be detected by means of FT-IR spectroscopy. The FT-IR spectrum of sample V7, prepared in air at 600 °C, showed the bands at 1018, 983 and 843 cm^{-1}, as well as a very broad band with peaks centered at 601, 519 and 486 cm^{-1}. In sample V8, produced at 600 °C in argon, additional bands at 951, 922, 884 and 738 cm^{-1} were observed that may be related to the formation of V_3O_7 as an associated phase in this sample.

Fig. 7 shows the Raman spectra of selected samples V0, V1, V7 and V8. The Raman bands observed for V_2O_5 are in line with literature data [15,16]. V0 showed all Raman bands as crystalline V_2O_5 samples; however, some of these bands were much broader than in crystalline sample, for example, those located at 283 and 302, 483 and 524, and 695 cm^{-1}. A band

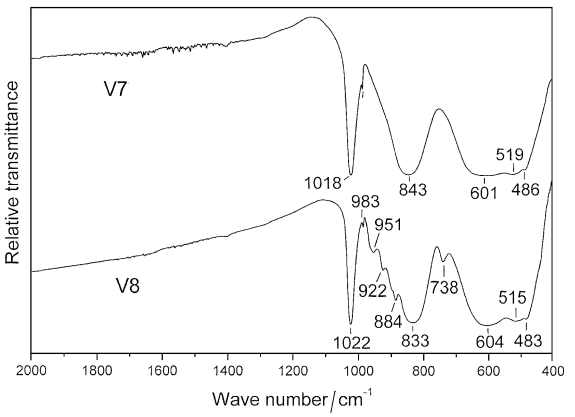

Fig. 6. FT-IR spectra of samples V7 and V8, produced by heating at 600 °C in air and argon, respectively. KBr matrix was used.

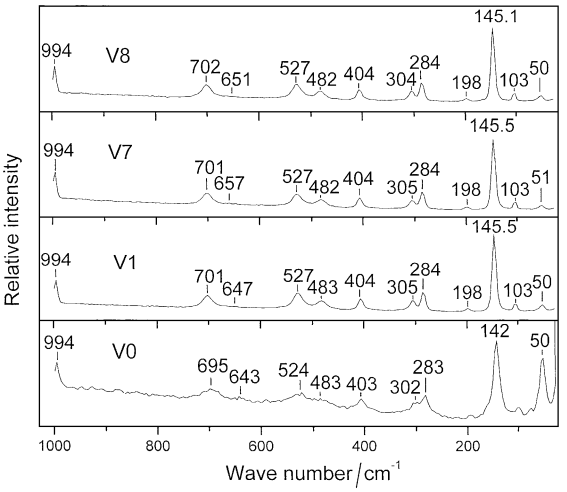

Fig. 7. Laser Raman spectra of samples V0, V1, V7 and V8.

of very small intensity at 643 cm^{-1} was also observed in sample V0, and it was shifted to 657 cm^{-1} for sample V7. This shift can be related with the crystal ordering of V_2O_5. Recently, Lee et al. [17] also observed Raman band at 650 cm^{-1} in amorphous V_2O_5 thin films and assigned it to the stretching vibration mode of V_2–O bond in a disordered V–O–V framework.

4. Conclusions

- Sol–gel procedure under well-defined experimental conditions was used to prepare V_2O_5. XRD showed an amorphous-like structure with a tendency to V_2O_5 crystallization, whereas TEM showed the presence of fibrillar particle morphology.
- The FT-IR spectrum of the starting V_2O_5 sample showed main features of the crystalline V_2O_5 spectrum, but not all bands typical of crystalline V_2O_5 were developed. On the other hand, the Raman spectrum of the starting V_2O_5 sample showed all bands of V_2O_5; however, they were significantly broader than in crystalline V_2O_5.
- Fibrillar morphology of the starting V_2O_5 particles was disappearing with an increase in heating temperature; this effect can be related to the release of water molecules, originally present in the particles. At 600 °C, big V_2O_5 particles of irregular shape were obtained. At 680 °C, the V_2O_5 glass transition was observed.
- Heating of the starting sample in argon atmosphere produced the V_3O_7 phase, beside the dominant V_2O_5 phase in that sample.

References

[1] O. Pelletier, P. Davidson, C. Bourgaux, C. Coulon, S. Regnault, J. Livage, Langmuir 16 (2000) 5295.
[2] S. Musić, N. Ljubešić, Colloid Polym. Sci. 258 (1980) 194.
[3] J.-J. Legendre, J. Livage, J. Colloid Interface Sci. 94 (1983) 75.
[4] J.-J. Legendre, P. Aldebert, N. Baffier, J. Livage, J. Colloid Interface Sci. 94 (1983) 84.
[5] H. Hirashima, M. Gengyo, C. Kojima, H. Imai, J. Non-Cryst. Solids 186 (1995) 54.
[6] A. Talledo, C.G. Granqvist, J. Appl. Phys. 77 (1995) 4655.
[7] E.A. Meulenkamp, W. Van Klinken, A.R. Schlatmann, Solid State Ionics 126 (1999) 235.
[8] N. Özer, Thin Solid Films 305 (1997) 80.
[9] G.T. Went, S. Ted Oyama, A.T. Bell, J. Phys. Chem. 94 (1990) 4240.
[10] N. Das, H. Eckert, H. Hu, I.E. Wachs, J.F. Walzer, F.J. Feher, J. Phys. Chem. 97 (1993) 8240.
[11] S. Kittaka, Y. Ayatsuka, K. Ohtani, N. Uchida, J. Chem. Soc., Faraday Trans. I 85 (1989) 3825.
[12] S. Kittaka, S. Sasaki, N. Ogawa, N. Uchida, J. Solid State Chem. 76 (1988) 40.
[13] P. Clauws, J. Wennik, Phys. Status Solidi, B 76 (1976) 707.
[14] P. Clauws, J. Broeckx, J. Wennik, Phys. Status Solidi, B 131 (1985) 459.
[15] C. Julien, G.A. Nazri, O. Bergström, Phys. Status Solidi, B 201 (1997) 319.
[16] V.V. Fomichev, P.I. Ukrainskaya, T.M. Ilyin, Spectrochim. Acta, A 53 (1997) 1833–1837.
[17] S.-H. Lee, H.M. Cheong, M.J. Seong, P. Liv, C.E. Tracy, A. Mascarenhas, J.R. Pitts, S.K. Deb, J. Appl. Phys. 92 (2002) 1893.